For submission to Surface Science

Surface-Catalyzed Dehydrogenation and Intermolecular C-C Bond Formation at Peripheral Alkyl Units on Cu(100) and Au(111)

Christopher G. Williams, ¹ Miao Wang, ² Jonathan P. Hopwood, ³ Christopher D. Tempas, ¹ Tobias W. Morris, ¹ David L. Wisman, ^{1,4} Larry L. Kesmodel, ² Jacob W. Ciszek, ³ and Steven L. Tait ^{1,2},*

¹Dept. of Chemistry and ²Dept. of Physics, Indiana University,
Bloomington, Indiana 47405, USA

³Dept. of Chemistry and Biochemistry, Loyola University Chicago, Chicago, Illinois 60660, USA

⁴ NAVSEA Crane, Crane, Indiana 47522, USA

* E-mail: <u>tait@indiana.edu</u>, Tel: +1-812-855-1302

Abstract

Hydrocarbon reactivity at surfaces has long been a topic of high interest for heterogeneous catalysis and is now gaining new importance for the development of surface nanostructures. To expand these structural libraries, molecules with larger functional groups are used on surfaces; these applications require the system to go to higher temperatures, necessitating studies of the reactivity and reaction pathways for alkyl type groups. We have designed and synthesized a prototypical molecule, 1,3,5-tris-(3,5-diethylphenyl)benzene

(TDEPB), to examine reactivity on Cu(100) and Au(111) surfaces using high resolution electron energy loss spectroscopy (HREELS) and scanning tunneling microscopy (STM). We report the dehydrogenation of ethyl groups in TDEPB at 450 K on Cu(100) and at 500 K on Au(111). For a structurally similar triphenylbenzene (TPB) molecule without the ethyl groups, dehydrogenation was only observed on the Cu(100) surface at 450 K. Desorption of TPB was observed from Au(111) at 500 K. For Au(111), it was thus the presence and reactivity of the ethyl groups that prevented complete desorption of the molecule. The reaction pathway for the ethyl groups was found to be different on Au(111) vs Cu(100), as two distinct steps were observed on Au(111). First, a dehydrogenation occurred at 500 K, followed by a structural change of the adsorbate at 550 K. The post-dehydrogenation structures on the two surfaces differ in the loss of the 750 cm⁻¹ HREELS feature on the Au(111) while not on Cu(100) and in other spectral changes for TDEPB on Cu(100) at 650 K that were not observed for TDEPB on Au(111) or for TPB on either surface. These results demonstrate reaction pathways that may be encountered with alkyl-functionalized molecular building blocks on surfaces at elevated temperatures.

Keywords

alkane dehydrogenation; C-C bond formation; catalysis; high-resolution electron energy loss spectroscopy; scanning tunneling microscopy; X-ray photoelectron spectroscopy

1. Introduction

Surface structure formation via C-C bond formation is a growing field due to the applications covalently linked surface structures have in catalysts, sensors, and electronics [1-5]. The most prevalent method for obtaining C-C bond formation is the use of halogens in Ullmann coupling. This type of linking has been utilized on a vast array of surface adsorbed species, such as small planar aromatic molecules (<C₁₈) [6-12], larger planar aromatic molecules (>C₁₈) [13-16], and porphyrins [17-20], leading to a large library of covalently-linked surface structures. Recently though, researchers have been exploring alternate pathways to obtain C-C linked species as the Ullmann coupling reaction produces free halogens and can leave behind strongly surface bonded byproducts [14, 15, 18, 21]. In previous work by our group [22], *intra*molecular dehydrocyclization was studied on Cu and in this study we seek to apply similar chemistry to *inter*molecular coupling on noble metal surfaces. The reaction pathway studied here is the dehydrogenation of the alkanes leading to the formation of a new molecular surface structure.

The use of unsaturated alkyl groups for surface mediated C-C bond formation has been recently explored with the use of ethynes [23-27]. More recent work on metal surfaces has looked into the use of alkene [28, 29] and alkanes [30, 31] in a surface reaction to enable C-C bond formation, but these studies were not designed to form extended surface structure. There are even fewer studies that use a sp³ C-H species in a dehydrogenative step for C-C bond structure formation on a surface [32]. Most work with the dehydrogenation of sp³ C-H species is typically done with (but not limited to) homogeneous Ir complexes [33-35], metal (Pt and Pt alloys) or metal-oxide (VO_x, MoO_x, GaO_x, InO_x, FeO_x, and CrO_x) substrates [36, 37], or more recently with metal-free catalysts [38-41]. Previous research has looked into the dehydrogenation of alkanes on metal surfaces, but few utilize vibration spectroscopy to observe the

dehydrogenation [37]. Our group has been able to observe the dehydrogenation of peripheral alkyl groups on organic molecules on Cu(100) at 500 K with HREELS [22].

Alkene coupling has been studied, but on-surface dehydrogenation can allow coupling of the simpler, saturated alkane starting materials by taking advantage of the catalytic activity of the surface. The work presented here addresses in situ dehydrogenation of peripheral ethyl groups on 1,3,5-tris-(3,5-diethylphenyl)benzene (TDEPB) (Scheme 1) on Cu(100) and Au(111) for the purpose of observing dehydrogenation and subsequent intermolecular C-C bond formation.

Scheme 1. Molecular structure of 1,3,5-tris-(3,5-diethylphenyl)benzene (TDEPB) and 1,3,5-triphenylbenzene (TPB).

2. Experimental

Cu(100) and Au(111) single crystals were purchased from Princeton Scientific. All experiments were conducted in ultra-high vacuum (UHV). In each experiment, the surface was cleaned by cycles of 1.5 keV Ar⁺ sputtering followed by thermal annealing at 730 K. Sample surface temperature was monitored by a thermocouple attached to the back side of the sample stage, which was calibrated to the surface temperature. The sample temperature was measured by a K-type thermocouple attached to the back side of the sample stage. In order to account for the

temperature difference between the sample surface and the stage, we conducted separate calibration experiments with a second thermocouple attached to the surface of a copper piece of the same size and mass as the single crystal used in the experiments reported here. Surface cleanliness was verified by the Auger electron spectroscopy (AES) metal to carbon signal ratio and by sharp LEED patterns. The surfaces were cooled gradually to room temperature before TDEPB or TPB vapor deposition in a separate but connected UHV chamber.

TDEPB was designed to maximize HREELS alkyl signal, avoid molecular desorption from the surface, provide multiple contacts between dehydrogenated species, and avoid intramolecular dehydrocyclization. TDEPB accomplished this by having multiple planar benzene rings and sufficient molecular weight to increase interaction with the surface and avoid desorption, thus allowing it to reach sufficient temperatures on the surface for dehydrogenation. Two ethyl groups were places on each peripheral benzene ring to have a large HREELS signal for observing alkane to alkene transition, while avoiding intramolecular C-C bond formation by positioning the alkanes in the 3 and 5 positions on each ring. Dehydrogenation followed by intermolecular bond formation or covalent binding to the surface would stabilize the molecules to even higher temperatures. TDEPB was synthesized via the triple condensation of 3.5diethylacetophenone using conditions similar to Zhang and coworkers [42]. Synthetic details and characterization can be found in the supplementary materials. Triphenylbenzene (TPB) was purchased from Sigma Aldrich (97% purity) for HREELS control experiments. Each molecule was degassed in UHV prior to deposition. Deposition was made from a Knudsen-type evaporator held at 390 K (TDEPB) or 385 K (TPB) to achieve a deposition rate of about 0.1 monolayers per minute, as monitored by quartz crystal microbalance. The surface coverage could not be verified using AES as the electron beam stimulated decomposition and desorption of the molecules. Submonolayer coverages were used to allow on-surface mobility of the molecules. Post-deposition annealing treatments were done in most experiments, as described below. For most of these annealing treatments, we chose an annealing time of 1.5 h to allow the system to reach a uniform chemical state to improve the HREEL spectra; longer annealing times did not lead to much further change (vide infra). We note that with this long anneal time, the temperatures reported do not represent a kinetic characterization of on-surface reactions, but do provide a relative measure of thermal activation between the different steps described herein.

High-resolution electron energy loss spectroscopy (HREELS) experiments were performed with a double-pass 127° angle cylindrical deflection electron spectrometer (LK Technologies, model LK 2000) operated at an incident beam energy of 5-8 eV and an elastic scattering peak width of 55 ± 10 cm⁻¹. Each spectrum was normalized by the average intensity of a featureless background region (1920-1950, 2630-2659, or 3693-3723 cm⁻¹) to account for variations in the primary beam current.

Scanning tunneling microscopy (STM) experiments were conducted in a separate UHV system than the HREELS experiments, but the sample preparation procedures, including cleaning and organic deposition, were the same. The STM system is also a multi-chamber system, with a dedicated chamber for organic deposition that is separate from the analysis chambers. Surface cleanliness was verified by X-ray photoelectron spectroscopy (XPS, SPECS GmbH XR-50 dual anode X-ray source and PHOIBOS 150 electron energy analyzer). STM (RHK Technologies SPM UHV 750) measurements were made at room temperature. The well-characterized (3 × 3) structure of terephthalic acid on the Cu(100) surface [43-45] was used to calibrate the STM. Sharp tungsten STM tips were fabricated by electrochemical etching. Bias voltages of 1.16 to 1.4 V (both polarities) and set point currents from 0.15 to 0.25 nA were

selected to find the best parameter for molecular resolution STM imaging. STM image analysis was conducted using the WSxM software [46].

3. Results and Discussion

3.1 Dehydrogenation on Cu(100)

TDEPB was vapor deposited on Cu(100) to a coverage of approximately 0.5 ML and analyzed by HREELS at various annealing steps. HREELS provided the surface sensitivity required to observe the vibrational changes to the surface adsorbate layer before and after the annealing. The most obvious features are at 758, 860, 1447, and 2953 cm⁻¹ with less predominant shoulders and features at 319, 471, 670, 1052, 1330, and 3041 cm⁻¹ (Table 1, Fig. 1). The HREEL spectra of TDEPB contained a low energy peak at 319 cm⁻¹ potentially due to a molecule-substrate interaction (Fig. S1). The out-of-plane peaks are observed at 471, 670, and 860 cm⁻¹ with the C-H out-of-plane bending mode at 758 cm⁻¹ (Table 1, Fig. 1). In-plane modes are observed at 1052 and 1330 cm⁻¹. The peak observed at 1447 cm⁻¹ is likely due to the alkane C-C stretch. The C-H stretching mode is composed of both sp³ and sp² carbon, which we identify at 2953 and 3041 cm⁻¹, respectively.

Table 1. HREELS peak assignments for TDEPB and TPB on each of Cu(100) and Au(111) after various annealing temperatures.

	TDEPB	TDEPB	TDEPB	TDEPB	TDEPB	TDEPB	TPB	TPB
	Cu(100)	Cu(100)	Cu(100)	Au(111)	Au(111)	Au(111)	Cu(100)	Au(111)
		500	K 650		500 K	550	K	
		anneal	anneal		anneal	anneal		
					(12.5 hrs) (17 ł	ırs)	
Out-of-plane Def.	319	319					297	
	471	464		486	486	501	486	494
	670	626	633		669		684	706
C-H Bendii	ng 758	758		747	743	757	758	747
Out-of-plane	860			864	846	860		860
Def.					948	985	941	
In-plane Def.	1052			1059				1073

							1175	1183
	1330	1345	1352	1293				
In-plane Wagging	C-H				1410	1381	1418	1476
Ethyl C-C Stretch	1447			1447				
In-plane	Def.						1579	1594
C-H	2953			2931	2967			
Stretching	3041	3041		3019	3019	3019	3055	3062

The substrate was annealed at various temperature steps for 1.5 h each and allowed to cool to room temperature for HREELS (Fig. 1). No significant change was observed after annealing up to 400 K, but significant changes are observed after annealing at 450 K. The C-H stretching mode decreased in intensity and changed shape, so that the peak centroid shifted from 2956 cm⁻¹ to 3006 cm⁻¹. The greater decrease in intensity on the low energy (2953 cm⁻¹) side of the peak compared to the high energy side (3041 cm⁻¹) indicates a preferential loss of sp³ C-H stretching [22, 47, 48]. Although a detailed mechanistic study is beyond the scope of this work, based on prior studies, we expect that the dehydrogenation should start at the more acidic allylic α carbon and then the β carbon [49], forming vinyl species that are capable of C-C bond formation [50]. We note that the longer anneal time here (1.5 h) allows a lower dehydrogenation temperature compared to our prior work with octaethyl porphyrin, which showed dehydrogenation at 500 K when annealed for 15 min [22].

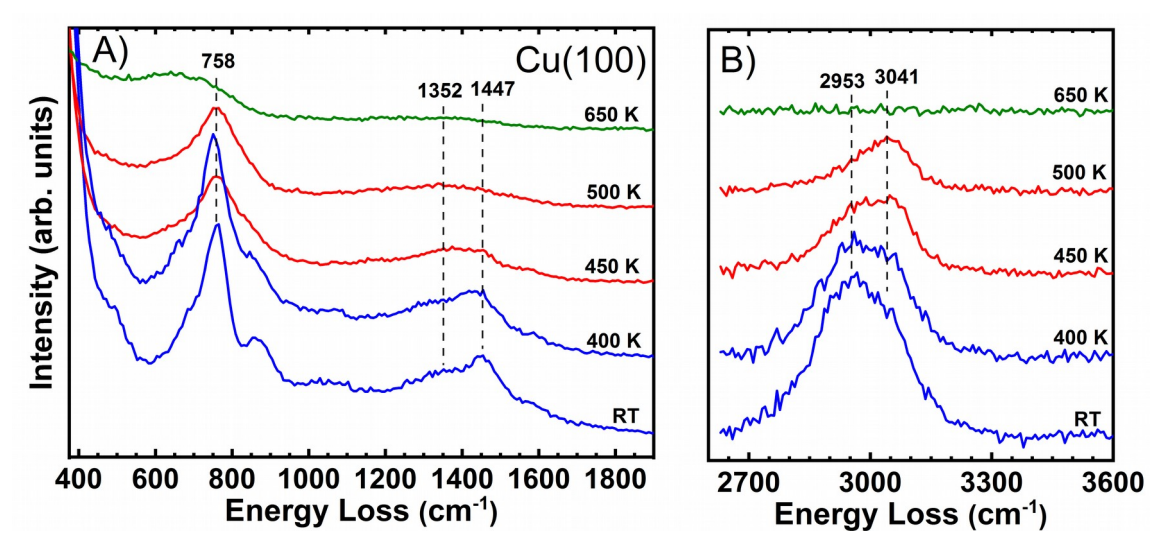


Fig. 1. HREELS of 0.5 ML of TDEPB on Cu(100) after annealing at 1.5 h at the temperature indicated and cooling to room temperature. TDEPB spectra are unchanged to 400 K (blue). At 450 K (red), there are noticeable intensity decreases in (A) C-C ethyl stretching mode at 1447 cm⁻¹ and (B) the lower half of the C-H stretching peak (2953 cm⁻¹), indicating ethyl dehydrogenation. At 650 K there was further C-H loss (green), so that few features remain in the HREEL spectrum, a result similar to prior measurements of a graphitic carbon layer on Rh [49]. Spectra in (B) are magnified 3x in intensity with respect to (A) for clarity of presentation.

Other changes were observed in the out-of-plane and in-plane vibrational modes. This is consistent with dehydrogenation as the loss of the sp³ C-H peak should coincide with the relative loss of the C-C features associated with the sp³ carbon, particularly the C-C stretching mode of the alkane at 1447 cm⁻¹. With annealing, the 471 cm⁻¹ peak broadens and shifts to a lower energy. The C-H out-of-plane bending mode at 758 cm⁻¹ remains present after annealing. The peaks within the in-plane region seem to remain close to their original position but do decrease in intensity. The alkane C-C stretching mode at 1447 cm⁻¹ significantly decreased in relative

intensity, as anticipated, and potentially leaves only in-plane modes left to be observed in this region. The spectra maintain these peak positions with annealing at 500 K.

At 650 K, there is a loss of the C-H bending mode at 758 cm⁻¹ and the appearance of a broad feature at 633 cm⁻¹. The remaining C-H stretching feature also seems to have fallen below our detection limits. The appearance of the broad peak at 633 cm⁻¹ and a broad feature of low intensity at 1352 cm⁻¹ matches the peak position and relative intensity for a graphitic layer on a Rh metal surface [49, 50].

STM images of 0.5 ML TDEPB on the Cu(100) surface at room temperature show some step edge decoration, but most of the molecules seem to be mobile (Fig. 2A). This is noted by the clear terraces and transient features (imaged as horizontal streaks) [51], which are attributed to molecules moving faster than the STM scan rate (2.9 lines per second). After annealing to 500 K, clear chains have formed across the surface (Fig. 2B). These chains indicate that a significant amount of C-C formation had occurred between molecules to form structures across the surface. This structural change coincides with the observed dehydrogenation temperature for the alkanes via HREELS. Thus, as the alkanes undergo dehydrogenation they are potentially forming C-C bonds to neighboring molecules until they become immobile on the surface. The structure of this species is similar to the oligomeric structure that is observed with alkyne linking on Cu surfaces [26, 27]. While the structures in their work did not undergo an initial dehydrogenation to form the structure, our linking reaction pathway is likely similar to other smaller molecular linking reactions on Cu surfaces where a dehydrogenation step occurs to allow for C-C bond formation [28, 30]. Our oligomeric structure results after this dehydrogenation and C-C bonding reaction due to the design of the TDEPB molecule. Further annealing at 680 K (above the observed HREELS change at 650 K) does not reveal any significant structural changes (Fig. 2C). What we

can conclude from the STM and HREELS data at this time is that the chemical change at 650 K leads to a near fully dehydrogenated chain-like carbonaceous structure across the Cu(100) surface. XPS shows the C peak area decreases by 20% indicating a change from 0.5 ML of TDEPB to 0.4 ML of TDEPB (Fig. S2).

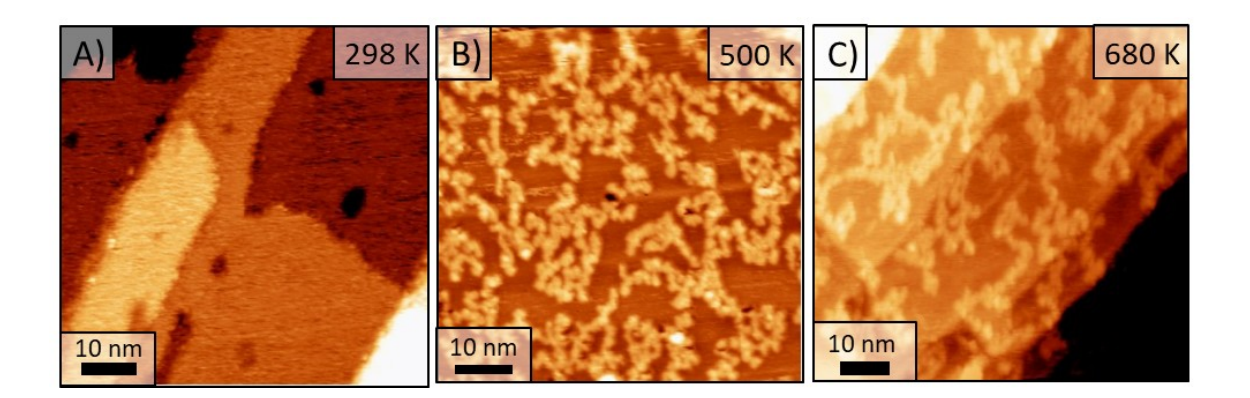


Fig. 2. STM of 0.5 ML of TDEPB on Cu(100) at (A) room temperature and after annealing to (B) 500 K and (C) 680 K. The sample was imaged at room temperature after each annealing step. Streaks in images indicate mobile molecules. (B) At 500 K, a structure forms due to intermolecular C-C bond formation. (C) 680 K saw little change to the long range order of the structure. STM bias and set point current were 1.16 V and 0.25 nA for (A, B) and -1.19 V and 0.18 nA for (C).

As a control, TPB (Scheme 1) was run through the same annealing procedure to observe what occurred in the absence of the alkane substituents. It is expected for TPB to have similar out-of-plane and in-plane mode positions as only the alkanes are absent. There are expected differences around the C-C stretching mode (above 1400 cm⁻¹) for alkane carbons and the sp³ C-H stretching modes for the alkane hydrogen. We observe no C-H stretching mode below 3000 cm⁻¹, consistent with the absence of sp³ carbon in TPB (Fig. 3). The position of the C-H peak in

TPB also aligns with the resulting peak in TDEPB after the annealing procedures (Fig. 4). This supports the expected thermally-induced dehydrogenation reaction of TDEPB to produce a higher fraction of sp² C-H species. However, there was an unexpected sharp peak for TPB at 1418 cm⁻¹ that is not observed for TDEPB. The strong intensity of this peak likely results from the mode having a strong dipole HREELS loss mechanism (a vibrational dipole more perpendicular to the surface). Off-specular analysis indicates that this mode is primarily a dipole scattering and oriented perpendicular to the surface; the percent change of the intensity is similar to other off-specular out-of-plane modes (684, 758, or 941 cm⁻¹) when compared to in-plane modes (1175 cm⁻¹) (Table S1). The position of this peak best aligns with in-plane C-H wagging modes on a benzene ring. In order for an in-plane ring mode to have a strong dipole loss mechanism the ring is either tilting on the Cu(100) surface causing the in-plane mode to now be more perpendicular to the surface, or the ring is interacting with the surface in a way that distorts the dipole of the vibrational mode to be more perpendicular to the surface.

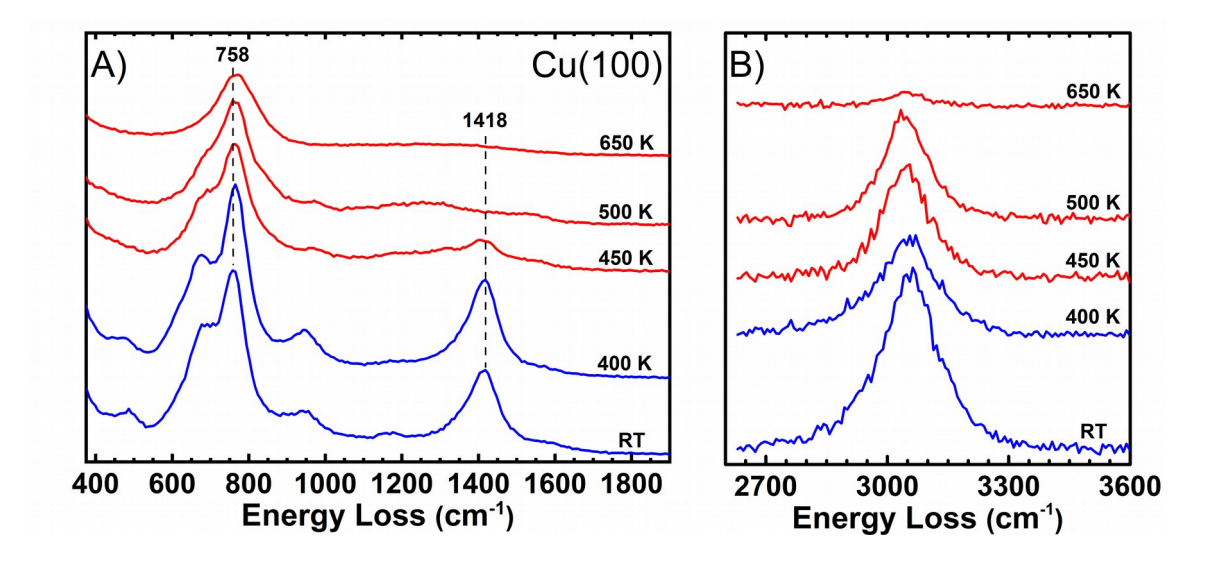


Fig. 3. HREELS of 0.4 ML of TPB on Cu(100) annealed to various temperatures. The surface was annealed for 1.5 h and was cooled to RT before each spectrum was acquired. (A) TPB remains predominantly the same until 400 K (blue). At 450 K we start to observe decreases to out-of-plane peaks and a decrease to the in-plane mode at 1418 cm⁻¹ (red). (B) C-H peak changes parallel those of the ring modes to indicate geometry changes of the molecule up to 500 K. The significant drop in C-H peak intensity from 500 K to 650 K is likely due to dehydrogenation as there is not an accompanying change in the ring modes. Spectra in (B) are magnified 2.5x with respect to (A).

The TPB showed behavior similar to the TDEPB when annealed: the in-plane and out-of-plane peaks start to change at 450 K. The C-H stretch peak area is observed to decrease slightly with each annealing step up to 500 K, then drops off sharply at higher temperatures. As aryl C-H bond scission is not anticipated below 500 K [22, 52-54], the changes to the peak area below 500 K are likely due to orientation changes of the phenyl rings with annealing so that they become more flat-lying. The C-H stretch position is consistent with sp² C-H and does not change through the annealing experiments. Note that TPB thermally desorbs from Au(111) at 500 K (see below), so the persistence of TPB on Cu(100) up to 650 K points to a chemical interaction to Cu, as

purely physisorbed interactions should be similar on those surfaces. The C-H peak area decrease above 500 K can thus be assigned to aryl dehydrogenation. While HREEL spectra for TDEPB and TPB both change with annealing they are likely due to different processes: TDEPB undergoes loss of the alkane C-C stretching mode and TPB has geometric changes to existing inplane vibrational modes with some aryl dehydrogenation at higher temperatures (Fig. 4). An interesting difference between the two molecules is observed at 650 K, where, for TPB (Fig. 3), a C-H peak (758 cm⁻¹) remains and a small C-H stretching mode is observable. The intermolecular linking of the TDEPB may prevent this ring tilting and thus keep more of the aryl C-H in closer contact with the surface.

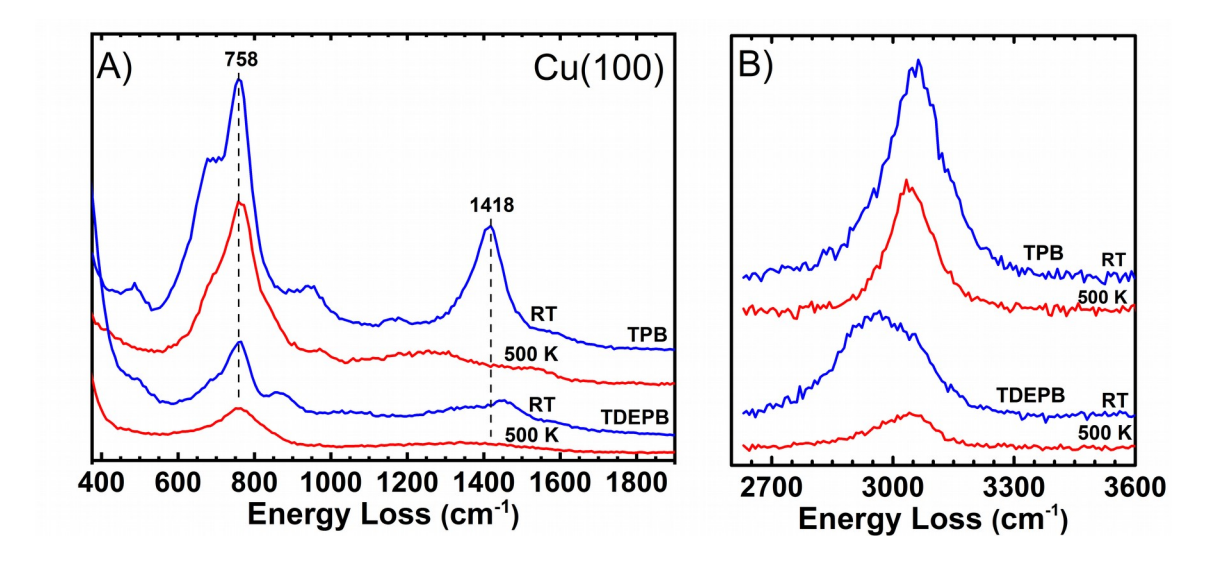


Fig. 4. HREELS comparison between 0.5 ML TDEPB and 0.4 ML TPB on the Cu(100) surface at RT (blue) and after their respective dehydrogenation (red). TDEPB shows loss of the ethyl C-C stretching peak at 1418 cm⁻¹ (A) and shift of the C-H peak to a sp² C-H species (B). There was additional observed decreases in intensity to other vibrational modes. TPB was observed to have a decrease to its in-plane mode at 1418 cm⁻¹ (A), decrease to C-H stretching mode (B), and similar changes to other out-of-plane modes where dehydrogenation is thought to occur. Spectra in (B) are magnified 3x with respect to (A).

We note a coverage dependence of the relative intensities of the vibrational modes for TPB (Fig. 5), particularly the in-plane C-H wagging mode at $1418 \, \text{cm}^{-1}$ increasing with coverage relative to the C-H bend at $758 \, \text{cm}^{-1}$. We attribute the increase in relative intensity to the phenyl rings tilting and π - π interactions with neighboring molecules at higher coverage. The rotated peripheral rings would change the relative intensity of the observed vibrational modes as the vibration dipoles change their orientation with respect to the surface. The higher coverage would also increase the frequency of phenyl ring interaction with other TPB molecules. The temperature where the aryl dehydrogenation is observed is not different between the higher and lower coverages of TPB, indicating that at these temperatures and coverages, all C-H bonds in TPB are able to interact with metal surface sites within the long anneal time, consistent with our observation, discussed above, of a transition to a more flat-lying orientation before dehydrogenation (Fig. 3). The overall nonlinear growth of vibrational mode intensity vs. coverage in Fig. 5 is due to screening effect of neighboring molecules, causing intensity saturation at high coverages, as observed in other HREELS studies [57, 58].

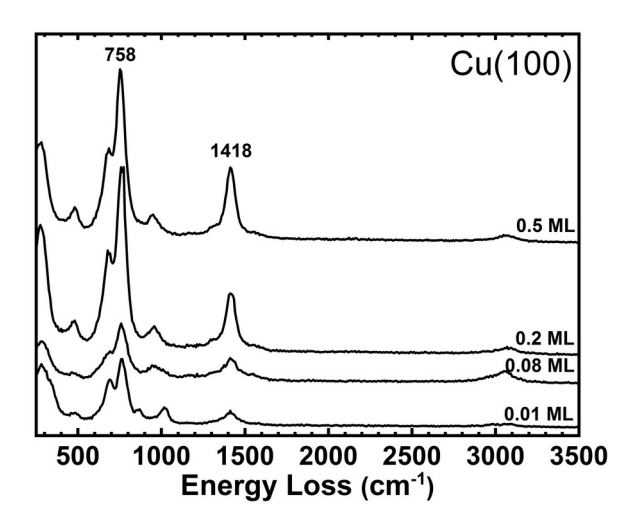


Fig. 5. HREEL spectra of increasing TPB coverage on Cu(100) surface at room temperature. We observe the increasing intensity of all the peaks with increasing coverage. There is a relative increase of the 1418 cm ⁻¹ C-H wagging peak compared to the C-H bend at 758 cm ⁻¹ from 0.27:1 to 0.44:1. We additionally observed a non-linear growth of the C-H peak.

3.2 Alkyl Dehydrogenation on Au(111)

For comparison to Cu(100), TDEPB was also studied on the Au(111) surface. We deposited 0.45 ML of TDEPB on Au(111) and annealed in temperature steps. HREEL spectra show little change up to 450 K, then significant changes by 550 K (Fig. 6). The C-H stretching mode shows some change at 500 K. This decrease coincided with a decrease to the alkane C-C stretching peak at 1447 cm⁻¹ while the other in-plane and out-of-plane modes did not change significantly, although there is some broadening of the right shoulder of the peak at 864 cm⁻¹. The spectra further changed with increasing annealing to 550 K. At this temperature, there was a significant drop in the lower half of the C-H stretching mode (centroid shift of 38 cm⁻¹ compared to room temperature). This change was seen as the dehydrogenation of the sp³ C-H species. After annealing at 550 K, there was a significant intensity decrease to the 747 cm⁻¹ peak and a decrease

of the ethyl C-C stretching mode (1447 cm⁻¹). On the other hand, the 864 cm⁻¹ out-of-plane mode intensity remains relatively constant, with some broadening to the peak. The spectra did not change significantly at higher temperatures. The out-of-plane modes over this annealing procedure had changed so that only a broad feature could be observed around 860 cm⁻¹ (different than Cu(100)), with a shoulder on the high energy side.

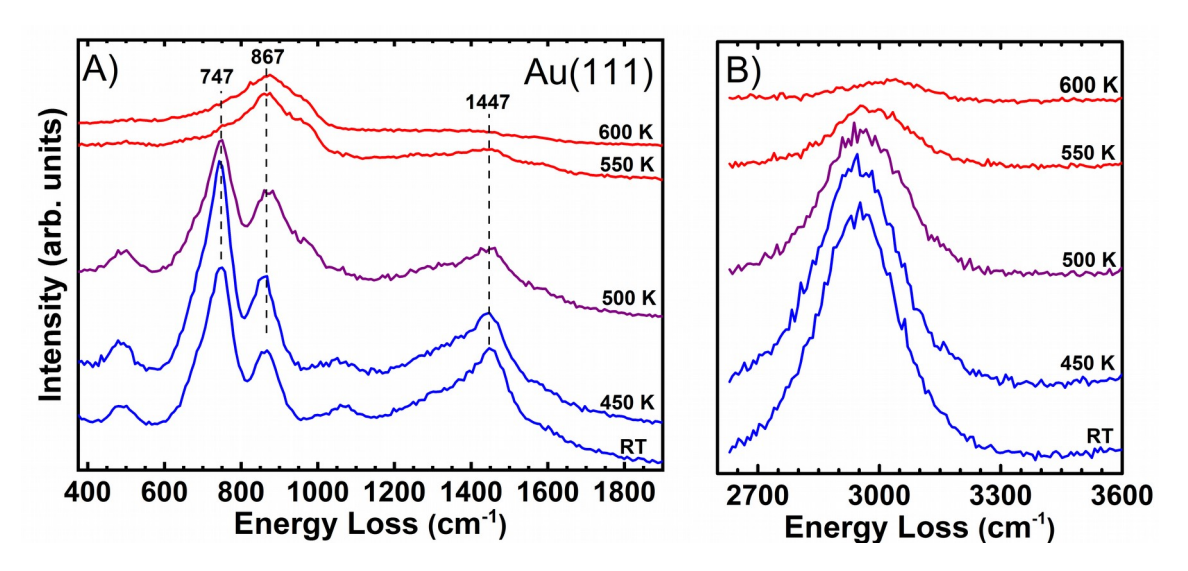


Fig. 6. HREEL spectra of 0.45 ML of TDEPB on Au(111) annealed to various temperatures. The sample was annealed at the temperature indicated for 1.5 h and allowed to cool to RT before each spectrum was acquired. The spectra do not change up to 450 K (blue), while annealing at 500 K causes some loss of the 747 cm⁻¹ out-of- plane peak, growth of a shoulder to the 867 cm⁻¹ peak, loss of the ethyl C-C stretching peak at 1447 cm⁻¹, and loss of intensity to the sp³ C-H peak area (purple). Further annealing increases these changes, resulting in a spectra with a prominent broad out-of-plane feature at 860 cm⁻¹, weak broad in-plane intensities, and what appears to be a purely sp² C-H species (red). Spectra in (B) are magnified 1.3x in intensity with respect to (A).

By increasing the annealing time of TDEPB on Au(111) at 500 and 550 K above 12 hours, we attempted to allow the reactions to proceed to completion (Fig. 7). This long anneal at

500 K produced a decrease in the C-C stretching mode at 1447 cm⁻¹ and in the sp² (lower energy) C-H stretching mode. There were other subtle changes to the out-of-plane and in-plane peak intensities but, for the most part, they remained relatively unchanged. These changes on Au(111) at 500 K are very similar to the dehydrogenation changes observed on the Cu(100).

After annealing TDEPB on Au(111) at 550 K, we observed a loss of the 747 cm⁻¹ out-of-plane peak, broadening of the out-of-plane peak at 860 cm⁻¹, and minimal changes to the in-plane mode, ethyl C-C, and the C-H stretching peak regions. These changes are not observed on Cu(100). The lack of C-H loss during this reaction step, but significant changes to the out-of-plane modes, point to a structural change to the adsorbate. This structural change is likely related to C-C bond formation between dehydrogenated ethyl species forming larger closed carbon ring systems; loss of the lower frequency out-of-plane bending mode that we observe here has been reported previously, *e.g.*, conversion of n-pentane to cyclopentane, n-hexane to cyclohexane, hexatriene to benzene, octane to cyclooctane, and 2-octene to cyclooctene [55].

The different annealing products for TDEPB on Cu(100) compared to Au(111) appear to have significant structural differences after dehydrogenation and C-C bonding. This different reactivity and structure between Cu and Au surfaces is consistent with previous work observing the Glaser coupling on these two surfaces [26]. In this previous work, alkyne coupling on Cu produced a variety of local bonding interactions involving two or three coupling units and leading to relatively disordered oligomeric structures [26, 27], while the Au surface facilitation cyclotrimerization (ring closing) to a much greater extent and produced highly ordered extended network structures [23, 25]. However, these studies did not involve a preceding dehydrogenation step.

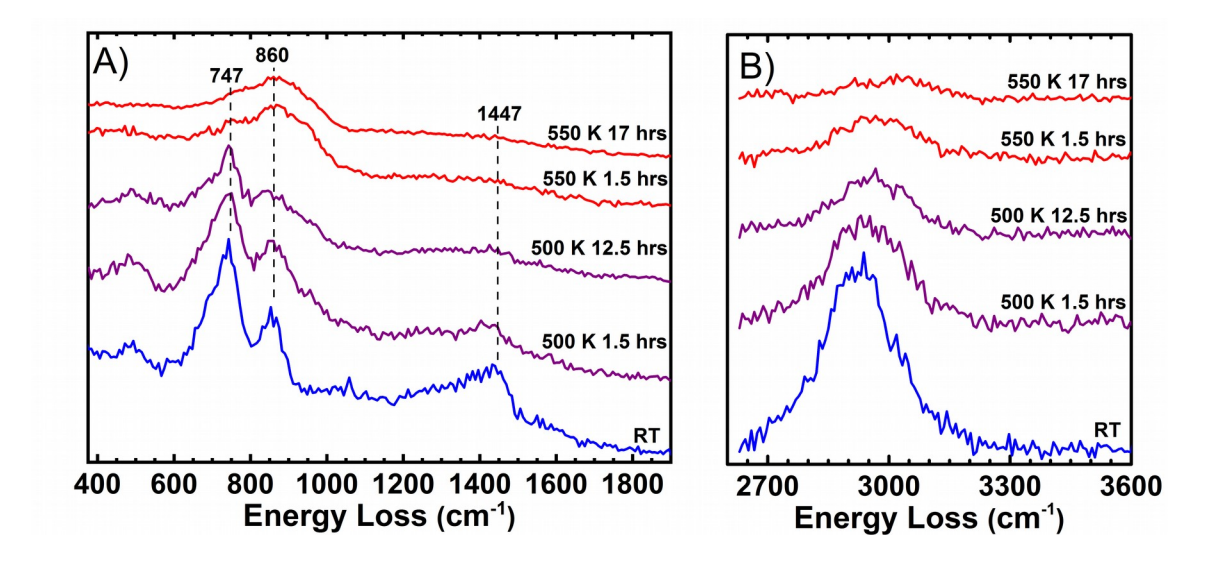


Fig. 7. HREELS of 0.45 ML of TDEPB on Au(111) annealed to various temperatures. Extended 12.5 h annealing at 500 K shows further dehydrogenation beyond what was accomplished in 1.5 h (purple). The peak at 747 cm⁻¹ is still visible after the majority of the dehydrogenation has taken place. Annealing to 550 K for 1.5 h causes the loss of this 747 cm⁻¹ peak while there little change to the in-plane modes, the position where the ethyl C-C stretching was located, or the C-H stretching peak intensity (red). The reaction process at 550 K is thus more of a structural change vs a significant dehydrogenation step. Annealing for longer times does not change the ring modes and only further dehydrogenation is observed (red). Spectra in (B) are magnified 2x in intensity with respect to (A).

STM of TDEPB on Au(111) revealed that at room temperature the molecules were mobile on the surface with some observable step edge decoration (Fig. 8). Streaks in the images, as for Cu(100), are due to TDEPB motion on the surface that is fast compared to the STM scan rate [51]. At 550 K, chain species began to form near step edges and these chains grew in abundance and length after annealing to 600 K, indicating C-C bond formation. There are still

streaks in STM images after annealing at 550 K and 600 K due to a mobile species. XPS indicates desorption of some of the TDEPB during annealing (Fig. S3).

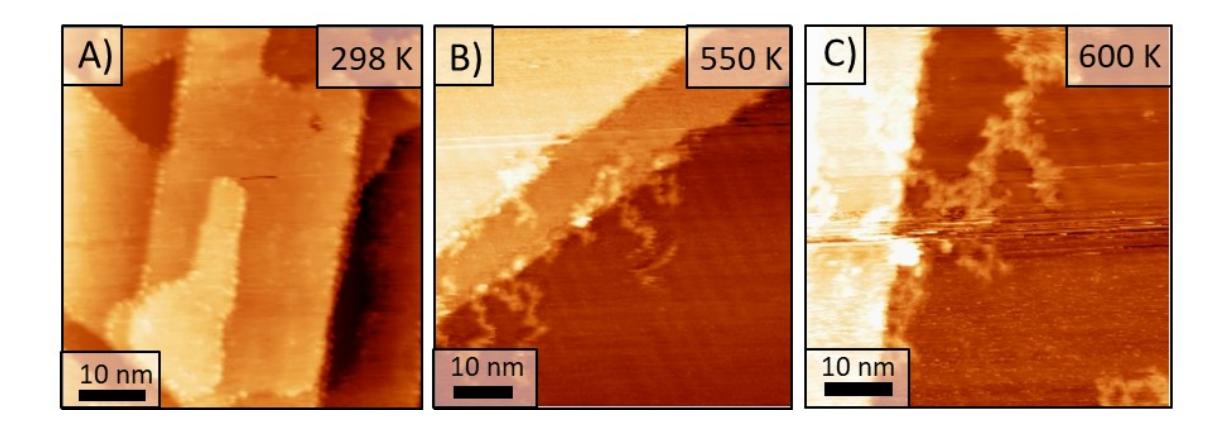


Fig. 8. STM of 0.9 ML of TDEPB on Au(111) annealed to various temperatures. (A) At room temperature, the is significant step edge decoration and some streaks in the images due to mobile molecules. (B) At 550 K, growth of chains, mostly at step edges, reveals C-C bond formation. (C) Annealing to 600 K causes further chain growth. XPS indicates a decrease in surface coverage to 0.4 ML after annealing to 550 K, but no further change at 600 K (Fig. S3). The herringbone pattern of Au(111) reconstruction is visible in parts of each image. Images were acquired at room temperature with 1.20-1.40 V bias and 0.15-0.19 nA setpoint current.

HREELS measurements of TPB on Au(111) show virtually no reactivity (Fig. 9).

Incremental TPB depositions were done to observe the TPB being slowly deposited onto the surface as noted by the increasing intensity of all the peaks. Upon reaching one monolayer the surface was heated to incrementally increasing temperatures. Deceasing intensity of TPB features started to occur at 500 K. When comparing the spectra of the low coverage TPB and the 1 ML spectra of the TPB after annealing at 500 K for 1.5 h, the peak shapes and intensity align

perfectly (Fig. S4). Thus, it was concluded that the observed changes to intensity result from molecular desorption and not from a reaction with the surface. The minor spectral differences at 1.0 ML (before annealing) relative to the lower coverage are likely due to differences in adsorption geometry, which revert upon annealing and thermal desorption. The lack of activity with TPB on Au(111) shows that the reactions observed with TDEPB are due to the ethyl species on the molecule and that the dehydrogenation of the ethyl groups is necessary to keep the molecule adsorbed to the surface.

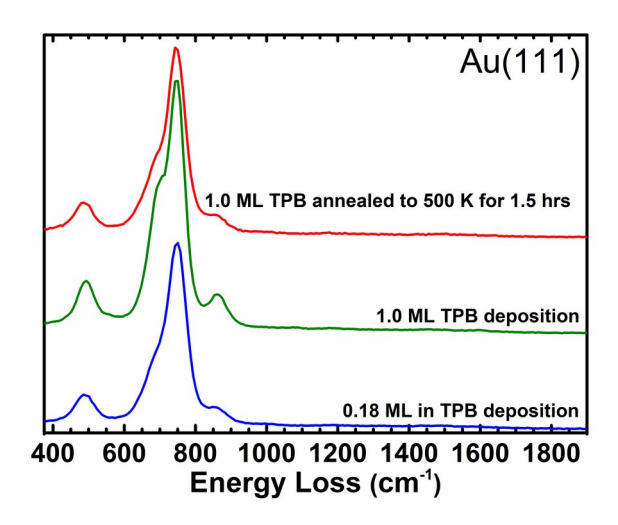


Fig. 9. HREELS of TPB on Au(111) at 0.18 ML (blue) and 1.0 ML (green) after room temperature deposition and after annealing 1.0 ML to 500 K for 1.5 h (red). Increasing intensity of all the peaks is observed with increasing coverage of TPB on the surface. After annealing 1 ML of the sample to 500 K (red) we saw a decrease to the intensities to match the submonolayer spectra (blue). This confirms that we have molecular desorption of TPB on the Au(111) surface with no reactions being observed.

4. Conclusion

Through the use of HREELS and STM we observed the dehydrogenation of ethyl groups in TDEPB on Cu(100) (450 K) and Au(111) (500 K). When studying a molecule without ethyl groups, TPB, dehydrogenation only occurred on the Cu(100). Desorption was observed on Au(111). For Au(111), the presence and reactivity of the ethyl groups in TDEPB prevented complete desorption of the molecule. The reactivity of the ethyl groups on Au(111) is suggested to occur in two distinct steps: a dehydrogenation at 500 K, followed by a possible structural change of the adsorbate at 550 K. The post-dehydrogenation structures on the Cu(100) and Au(111) surfaces were viewed as being different due to the loss of the 750 cm⁻¹ mode on the Au(111). At higher temperature (650 K) on Cu(100), a subsequent reaction leads to further C-H loss. This process did not occur with TDEPB on Au(111) or with TPB on any surface. STM revealed that, while initially mobile on the surfaces, after the dehydrogenation of TDEPB, possible C-C bonds formed chain-like features across the surface. Reactivity studies such as the ones shown here are required to understand how larger molecules utilizing organizing species like alkane chains may behave at higher temperatures. We also show the use of different surfaces and the use of ethyl groups can change the final observed dehydrogenated structure.

5. Acknowledgements

Surface analysis experiments at Indiana University were supported by the U. S. Department of Energy, Office of Basic Energy Sciences, Chemical Sciences program, DE-SC0016367. TDEPB synthesis at Loyola University Chicago was supported by the National Science Foundation (NSF), award No. 1665433.

6. References

- [1] H. Klauk, Organic Electronics: Materials, Manufacturing, and Applications, John Wiley & Sons, Weinheim, 2006.
- [2] I. Mochida, K. Suetsugu, H. Fujitsu, K. Takeshita, Enhanced catalytic activity of cobalt tetraphenylporphyrin on titanium dioxide by evacuation at elevated temperatures for intensifying the complex-support interaction, J. Phys. Chem., 87 (1983) 1524-1529.
- [3] J.W. Colson, W.R. Dichtel, Rationally synthesized two-dimensional polymers, Nat Chem, 5 (2013) 453-465.
- [4] Q. Shen, H.Y. Gao, H. Fuchs, Frontiers of on-surface synthesis: From principles to applications, Nano Today, 13 (2017) 77-96.
- [5] P.A. Held, H. Fuchs, A. Studer, Covalent-Bond Formation via On-Surface Chemistry, Chem. Eur. J., 23 (2017) 5874-5892.
- [6] A. Basagni, F. Sedona, C.A. Pignedoli, M. Cattelan, L. Nicolas, M. Casarin, M. Sambi, Molecules—oligomers—nanowires—graphene nanoribbons: A bottom-up stepwise on-surface covalent synthesis preserving long-range order, J. Am. Chem. Soc., 137 (2015) 1802-1808.
- [7] C. Zhang, Q. Sun, H. Chen, Q. Tan, W. Xu, Formation of polyphenyl chains through hierarchical reactions: Ullmann coupling followed by cross-dehydrogenative coupling, Chem. Commun., 51 (2015) 495-498.
- [8] M.M. Blake, S.U. Nanayakkara, S.A. Claridge, L.C. Fernández-Torres, E.C.H. Sykes, P.S. Weiss, Identifying reactive intermediates in the Ullmann coupling reaction by scanning tunneling microscopy and spectroscopy, J. Phys. Chem. A, 113 (2009) 13167-13172.
- [9] A.R. Lahrood, J. Björk, W.M. Heckl, M. Lackinger, 1, 3-Diiodobenzene on Cu (111)—an exceptional case of on-surface Ullmann coupling, Chem. Commun., 51 (2015) 13301-13304.

- [10] T.A. Pham, F. Song, M.T. Nguyen, Z. Li, F. Studener, M. Stöhr, Comparing Ullmann Coupling on Noble Metal Surfaces: OnSurface Polymerization of 1, 3, 6, 8Tetrabromopyrene on Cu (111) and Au (111), Chem. Eur. J., 22 (2016) 5937-5944.
- [11] J. LiptonDuffin, O. Ivasenko, D. Perepichka, F. Rosei, Synthesis of polyphenylene molecular wires by surface confined polymerization, Small, 5 (2009) 592-597.
- [12] E. Lewis, C. Murphy, A. Pronschinske, M. Liriano, E. Sykes, Nanoscale insight into C–C coupling on cobalt nanoparticles, Chem. Commun., 50 (2014) 10035-10037.
- [13] J. Cai, P. Ruffieux, R. Jaafar, M. Bieri, T. Braun, S. Blankenburg, M. Muoth, A.P. Seitsonen, M. Saleh, X. Feng, K. Mullen, R. Fasel, Atomically Precise Bottom-up Fabrication of Graphene Nanoribbons, Nature, 466 (2010) 470-473.
- [14] M. Bieri, M. Treier, J.M. Cai, K. Ait-Mansour, P. Ruffieux, O. Groning, P. Groning, M. Kastler, R. Rieger, X.L. Feng, K. Mullen, R. Fasel, Porous graphenes: two-dimensional polymer synthesis with atomic precision, Chem. Commun., 0 (2009) 6919-6921.
- [15] R. Gutzler, H. Walch, G. Eder, S. Kloft, W.M. Heckl, M. Lackinger, Surface mediated synthesis of 2D covalent organic frameworks: 1,3,5-tris(4-bromophenyl)benzene on graphite(001), Cu(111), and Ag(110), Chem. Commun., 0 (2009) 4456-4458.
- [16] J. Eichhorn, D. Nieckarz, O. Ochs, D. Samanta, M. Schmittel, P.J. Szabelski, M. Lackinger, On-Surface Ullmann Coupling: The Influence of Kinetic Reaction Parameters on the Morphology and Quality of Covalent Networks, ACS Nano, 8 (2014) 7880-7889.
- [17] L. Lafferentz, V. Eberhardt, C. Dri, C. Africh, G. Comelli, F. Esch, S. Hecht, L. Grill, Controlling on-surface polymerization by hierarchical and substrate-directed growth, Nat Chem, 4 (2012) 215-220.

- [18] L. Grill, M. Dyer, L. Lafferentz, M. Persson, M.V. Peters, S. Hecht, Nano-architectures by covalent assembly of molecular building blocks, Nat. Nanotechnol., 2 (2007) 687-691.
- [19] J. Beggan, N. Boyle, M. Pryce, A. Cafolla, Surface-confined Ullmann coupling of thiophene substituted porphyrins, Nanotechnology, 26 (2015) 365602.
- [20] G. Kuang, Q. Zhang, D.Y. Li, X.S. Shang, T. Lin, P.N. Liu, N. Lin, Cross Coupling of Aryl Bromide and PorphyrinBromide on an Au (111) Surface, Chem. Eur. J., 21 (2015) 8028-8032.
- [21] L. Dong, P.N. Liu, N. Lin, Surface-activated coupling reactions confined on a surface, Acc. Chem. Res., 48 (2015) 2765-2774.
- [22] C.G. Williams, M. Wang, D. Skomski, C.D. Tempas, L.L. Kesmodel, S.L. Tait, Dehydrocyclization of peripheral alkyl groups in porphyrins at Cu (100) and Ag (111) surfaces, Surf. Sci., 653 (2016) 130-137.
- [23] H. Zhou, J. Liu, S. Du, L. Zhang, G. Li, Y. Zhang, B.Z. Tang, H.J. Gao, Direct visualization of surface-assisted two-dimensional diyne polycyclotrimerization, J Am Chem Soc, 136 (2014) 5567-5570.
- [24] F. Xiang, Y. Lu, C. Li, X. Song, X. Liu, Z. Wang, J. Liu, M. Dong, L. Wang, Cyclotrimerization-Induced Chiral Supramolecular Structures of 4-Ethynyltriphenylamine on Au(111) Surface, Chemistry, 21 (2015) 12978-12983.
- [25] J. Liu, P. Ruffieux, X. Feng, K. Mullen, R. Fasel, Cyclotrimerization of arylalkynes on Au(111), Chemical communications, 50 (2014) 11200-11203.
- [26] H.Y. Gao, H. Wagner, D. Zhong, J.H. Franke, A. Studer, H. Fuchs, Glaser coupling at metal surfaces, Angew Chem Int Ed Engl, 52 (2013) 4024-4028.

- [27] J. Eichhorn, W.M. Heckl, M. Lackinger, On-surface polymerization of 1,4-diethynylbenzene on Cu(111), Chemical communications, 49 (2013) 2900-2902.
- [28] Q. Sun, L. Cai, Y. Ding, L. Xie, C. Zhang, Q. Tan, W. Xu, Dehydrogenative homocoupling of terminal alkenes on copper surfaces: a route to dienes, Angew Chem Int Ed Engl, 54 (2015) 4549-4552.
- [29] K.-J. Shi, C.-H. Shu, C.-X. Wang, X.-Y. Wu, H. Tian, P.-N. Liu, On-Surface Heck Reaction of Aryl Bromides with Alkene on Au(111) with Palladium as Catalyst, Org. Lett., 19 (2017) 2801-2804.
- [30] L. Cai, Q. Sun, C. Zhang, Y. Ding, W. Xu, Dehydrogenative homocoupling of alkyl chains on Cu (110), Chemistry-A European Journal, 22 (2016) 1918-1921.
- [31] Z. Cai, M. Liu, L. She, X. Li, J. Lee, D.-X. Yao, H. Zhang, L. Chi, H. Fuchs, D. Zhong, Linear Alkane C-C Bond Chemistry Mediated by Metal Surfaces, ChemPhysChem, 16 (2015) 1356-1360.
- [32] X. Leng, Y. Lu, G. Feng, Z. Wang, W. Li, X. Liu, R. Zhang, N. Zhang, L. Wang, Surface-assisted dehydrogenative homocoupling and cyclodehydrogenation of mesityl groups on a copper surface, Chemical communications, 53 (2017) 9151-9154.
- [33] F. Liu, E.B. Pak, B. Singh, C.M. Jensen, A.S. Goldman, Dehydrogenation of n-alkanes catalyzed by iridium "pincer" complexes: regioselective formation of α-olefins, J. Am. Chem. Soc., 121 (1999) 4086-4087.
- [34] R.H. Crabtree, J.M. Mihelcic, J.M. Quirk, Iridium complexes in alkane dehydrogenation, J. Am. Chem. Soc., 101 (1979) 7738-7740.
- [35] C. Gunanathan, D. Milstein, Applications of acceptorless dehydrogenation and related transformations in chemical synthesis, Science, 341 (2013) 1229712.

- [36] B.M. Weckhuysen, R.A. Schoonheydt, Alkane dehydrogenation over supported chromium oxide catalysts, Catal. Today, 51 (1999) 223-232.
- [37] J.J.H.B. Sattler, J. Ruiz-Martinez, E. Santillan-Jimenez, B.M. Weckhuysen, Catalytic Dehydrogenation of Light Alkanes on Metals and Metal Oxides, Chem. Rev., 114 (2014) 10613-10653.
- [38] J. Zhang, X. Liu, R. Blume, A. Zhang, R. Schlögl, D.S. Su, Surface-modified carbon nanotubes catalyze oxidative dehydrogenation of n-butane, Science, 322 (2008) 73-77.
- [39] J. Zhang, X. Wang, Q. Su, L. Zhi, A. Thomas, X. Feng, D.S. Su, R. Schlögl, K. Müllen, Metal-free phenanthrenequinone cyclotrimer as an effective heterogeneous catalyst, J. Am. Chem. Soc., 131 (2009) 11296-11297.
- [40] B. Frank, J. Zhang, R. Blume, R. Schlögl, D.S. Su, Heteroatoms increase the selectivity in oxidative dehydrogenation reactions on nanocarbons, Angew. Chem. Int. Ed., 48 (2009) 6913-6917.
- [41] J.T. Grant, C.A. Carrero, F. Goeltl, J. Venegas, P. Mueller, S.P. Burt, S.E. Specht, W.P. McDermott, A. Chieregato, I. Hermans, Selective oxidative dehydrogenation of propane to propene using boron nitride catalysts, Science, 354 (2016) 1570-1573.
- [42] S.-L. Zhang, Z.-F. Xue, Y.-R. Gao, S. Mao, Y.-Q. Wang, Triple condensation of aryl methyl ketones catalyzed by amine and trifluoroacetic acid: straightforward access to 1,3,5-triarylbenzenes under mild conditions, Tetrahedron Letters, 53 (2012) 2436-2439.
- [43] S. Stepanow, T. Strunskus, M. Lingenfelder, A. Dmitriev, H. Spillmann, N. Lin, J.V. Barth, C. Wöll, K. Kern, Deprotonation-driven phase transformations in terephthalic acid self-assembly on Cu(100), J. Phys. Chem. B, 108 (2004) 19392-19397.

- [44] S.L. Tait, Y. Wang, G. Costantini, N. Lin, A. Baraldi, F. Esch, L. Petaccia, S. Lizzit, K. Kern, Metal-organic coordination interactions in Fe-terephthalic acid networks on Cu(100), J. Am. Chem. Soc., 130 (2008) 2108-2113.
- [45] Y. Ge, H. Adler, A. Theertham, L.L. Kesmodel, S.L. Tait, Adsorption and Bonding of First Layer and Bi-layer Terephthalic Acid on the Cu(100) Surface by High-Resolution Electron Energy Loss Spectroscopy, Langmuir, 26 (2010) 16325-16329.
- [46] I. Horcas, R. Fernandez, J.M. Gomez-Rodriguez, J. Colchero, J. Gomez-Herrero, A.M. Baro, WSXM: A software for scanning probe microscopy and a tool for nanotechnology, Rev. Sci. Instr., 78 (2007) 013705.
- [47] A.V. Teplyakov, B.E. Bent, J. Eng Jr, J.G. Chen, Vibrational Mode-softening of Alkanes on Clean and Modified Cu and Mo Surfaces: Absence of a Simple Correlation with Thermal Desorption Temperatures, Surf. Sci., 399 (1998) L342-L350.
- [48] H. Ogoshi, N. Masai, Z. Yoshida, J. Takemoto, K. Nakamoto, The Infrared Sprectra of Metallooctaehtyl Porphyrins, Bull. Chem. Soc. Jpn., 44 (1971) 3.
- [49] B. Koel, J. Crowell, B. Bent, C. Mate, G. Somorjai, Thermal decomposition of benzene on the rhodium (111) crystal surface, J. Phys. Chem., 90 (1986) 2949-2956.
- [50] M.-C. Wu, Q. Xu, D.W. Goodman, Investigations of Graphitic Overlayers Formed from Methane Decomposition on Ru (0001) and Ru (11. hivin. 20) Catalysts with Scanning Tunneling Microscopy and High-Resolution Electron Energy Loss Spectroscopy, J. Phys. Chem., 98 (1994) 5104-5110.
- [51] G. Antczak, K. Boom, K. Morgenstern, Revealing the Presence of Mobile Molecules on the Surface, J. Phys. Chem. C, 121 (2016) 542-549.

- [52] Q. Sun, C. Zhang, L. Cai, L. Xie, Q. Tan, W. Xu, On-surface Formation of Two-dimensional Polymer via Direct C-H Activation of Metal Phthalocyanine, Chem. Commun., 51 (2015) 2836-2839.
- [53] Q. Sun, C. Zhang, H. Kong, Q. Tan, W. Xu, On-surface aryl–aryl coupling via selective C–H activation, Chem. Commun., 50 (2014) 11825-11828.
- [54] S. Haq, F. Hanke, J. Sharp, M. Persson, D.B. Amabilino, R. Raval, Versatile Bottom-Up Construction of Diverse Macromolecules on a Surface Observed by Scanning Tunneling Microscopy, ACS Nano, 8 (2014) 8856-8870.
- [55] NIST Mass Spec Data Center, S. E. Stein, director, Infrared Spectra, in: P.J. Linstrom, W.G. Mallard (Eds.) NIST Chemistry WebBook, NIST Standard Reference Database Number 69, National Institute of Standards and Technology, Gaithersburg MD, 20899, DOI: 10.18434/T4D303, (retrieved November 15, 2017).